View Journal

Nanoscale Advances

Accepted Manuscript

This article can be cited before page numbers have been issued, to do this please use: N. W. Pech-May and M. Retsch, *Nanoscale Adv.*, 2019, DOI: 10.1039/C9NA00557A.

View Article Online
DOI: 10.1039/C9NA00557A

Tunable daytime passive radiative cooling based on a broadband angle selective low-pass filter

Nelson W. Pech-May[1,*] and Markus Retsch[1,†]

[1] *Department of Chemistry, University of Bayreuth, Universitätsstr. 30, 95447 Bayreuth, Germany*

(Dated: October 12, 2019)

Passive daytime cooling could contribute to a reduction of our global energy consumption. It is capable of cooling materials down to below ambient temperatures without the necessity of any additional input energy. Yet, current devices and concepts all lack the possibility to switch the cooling properties on and off. Here, we introduce a dynamic control for passive radiative cooling during daytime. Using an angle-selective solar filter on top of a nocturnal passive radiator, allows tuning the surface temperature of the later in a wide range by just tilting the filter from normal incidence up to around 23 °. This angle-selective filter is based on optically engineered, one-dimensional photonic crystal structures. We use numerical simulations to investigate the feasibility of a switchable low-pass filter/emitter device.

INTRODUCTION

Daytime passive radiative cooling has recently gained attention due to its high potential for cooling surfaces even when exposed to solar radiation.[1–5] Ideally, this technology can cool surfaces even below the ambient temperature without any external power input. Complementary, nocturnal passive radiative coolers, which have been studied since the 1970's, can only produce net cooling during night, when the cooling material is not exposed to solar radiation.[6, 7] The physical mechanism responsible of passive radiative cooling is based on the exchange of heat by radiation between a surface or body (at around 300 K) on the surface of the earth and the outer space, which is cold (at around 2.8 K). To exchange heat by radiation, this surface must show high emissivity within the sky-window: $7.5 \leq \lambda \leq 14$ μm.[1] The reason is, that this spectral range coincides with one of the transparent bands of the atmosphere. Moreover, the blackbody radiation of a surface at temperature $\sim$ 300 K peaks in the same spectral range. Briefly, a surface with high emissivity within the sky-window will passively cool itself by radiative heat transfer to the cold outer space. This principle is applied for cooling during night. However, during daytime, the solar radiation must be reflected or scattered effectively to cool down a surface.

Various approaches have been proposed to obtain daytime passive radiative coolers, including photonic structures,[4] microparticles embedded in a polymer,[5] hierarchically porous polymers,[3] complete delignification and densification of wood,[8] among others. Nevertheless, all of these very different approaches are only able to produce fixed amounts of cooling power, unchangeable once their intrinsic characteristics are determined by the material design. In practice, it would be desirable to control the cooling (or heating) power of a device at will, such as in a fridge or an air-conditioner. Additionally, depending on the year's season one would need heating (in winter) or cooling (in summer) power to maintain a comfortable room temperature.

One way to tune the cooling power during daytime consists in gaining dynamic control over the reflection of the solar spectrum. In this way, one would account for the amount of radiated power from the sun that could be absorbed by the radiator surface. It was only until 2014, when the group of J. Joannopoulos demonstrated a broadband reflector with angular selectivity.[9]

Angle selectivity in 1D photonic crystals is based on the zero reflection occurring at the interface between two media with p-polarized light at the Brewster angle, which is usually larger than 45 °.[9, 10] This angle is specific for each wavelength. To achieve broadband applicability, multiple periodicity in the 1D stratified structure is needed.[9, 11] Up to now, research has been focused on studying angle-selective broadband filters in the visible range, considering mainly $p-$polarized light. Nevertheless, the design of an angle-selective solar filter must consider both polarization states ($s-$polarized and $p-$polarized light). This is critical because, solar radiation is mostly unpolarized. To fulfill this condition, the filter components should be impedance-matched with the surrounding air.[9] Moreover, another advantage of impedance-matching with air is that in this case, the Brewster angle occurs at normal incidence. Here, we have combined both approaches: impedance-matching [9] for angle selectivity around normal incidence (valid for both polarization states) and broadband reflectivity [11] from 1D stratified stacks of multiple periodicity, to successfully design an angle-selective solar filter.

In this work, we propose an angle-selective solar filter on top of a nocturnal passive radiative surface, to achieve tunable radiative cooling (or heating) power during daytime. The impedance-matched filter serves as active control of the reflected solar radiation, while the nocturnal radiator cools itself by thermal emission through the sky-window. The components of the 1D stratified structure need to be transparent in the sky-window range to allow transmission of the radiator. Numerical simulations performed considering 298.3 K atmospheric temperature show that the radiator surface can be tuned from 270 K to 352 K by just tilting the solar filter from normal incidence

View Article Online
DOI: 10.1039/C9NA00557A 2

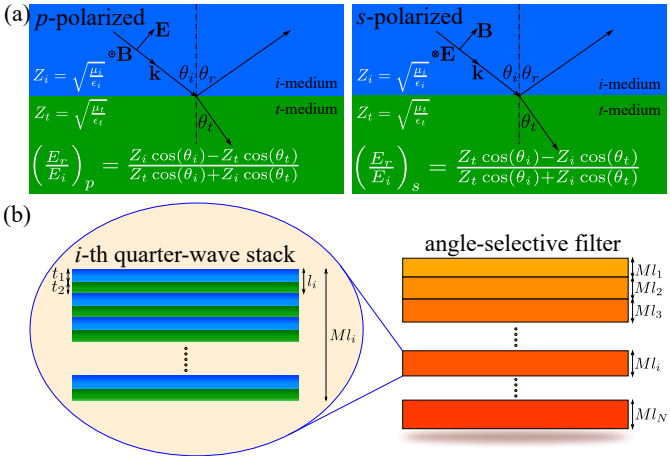

FIG. 1. Geometry of a broadband angle selective filter based in N quarter-wave stacks of increasing thickness. Each quarter-wave stack is conformed by M bilayers satisfying the Bragg condition.

(0 °) up to around 23 °. The designed filter consists of 75 quarter-wave stacks of geometrically increasing periodicity, each one composed of 64 unit-cells or bilayers. The characteristics of the filter have been tailored using the Transfer-Matrix Method to compute the transmittance spectra.[12, 13] On the other hand, the nocturnal radiator consists of a microstructured silica photonic crystal which is also a solar absorber.[2] This radiator has been chosen to prove the cooling (or heating) tunability enabled by the proposed filter-radiator device. Moreover, our results show that controlling the reflection of the solar radiation with a filter, instead of the static approach in daytime passive radiative cooling (structuring the radiator surface itself to reflect or scatter the solar radiation) paves the way to achieve a tunable passive radiative cooling during daytime.

CONCEPT OF AN ANGLE-SELECTIVE FILTER FOR THE SOLAR SPECTRUM

We introduce a 1D photonic device to model a broadband filter that covers the whole solar spectrum ($0.26\,\mu\text{m} \leq \lambda \leq 2.5\,\mu\text{m}$). The aim of this filter is to transmit electromagnetic waves with wavelengths longer than 2.5 μm and to reflect all incoming waves with wavelengths within the solar spectrum. Moreover, this filter operates as described for any state of polarization of the incoming waves and above a given angle of incidence.

Consider an incidence medium ($i-$medium) of refractive index $n_i = \sqrt{\epsilon_i \mu_i}$ in contact with a transmittance medium ($t-$medium) of refractive index $n_t = \sqrt{\epsilon_t \mu_t}$. Where, ϵ_x is the electric permitivity and μ_x the magnetic permeability of each medium $x = \{i, t\}$. Figure 1a shows the reflectivity equations, i.e, the ratio between the magnitudes of the reflected electric field (E_r) and the incident electric field (E_i), for both $s-$ and $p-$polarized incident light. The incident electromagnetic (EM) waves, with electric field $\mathbf{E}$ and magnetic field $\mathbf{B}$, have wavevector $\mathbf{k}$ with incident angle θ_i. The direction of the reflected and transmitted EM waves is characterized by the reflectance angle ($\theta_r = \theta_i$) and transmittance angle (θ_t), respectively. The reflection fields at the boundary between these two media are given by the well-known Fresnel equations.[14] These expressions show that the impedance of each medium governs the reflectivity. In particular, for impedance-matched media ($Z_i = Z_t$): reflection becomes zero at both polarization states for $\cos\theta_i = \cos\theta_t$. This is satisfied when the incidence angle θ_i equals the transmittance angle θ_t. Therefore, the zero reflection condition at the boundary of two impedance-matched media with different refractive indices is only satisfied for normal incidence: $\theta_i = \theta_t = 0$, as can be inferred from Snell's law ($n_i \sin\theta_i = n_t \sin\theta_t$).

It has been shown in literature that reflection over a broadband frequency range can be obtained by piling up two or more 1D photonic crystals of appropriate periodicities.[10, 11] Accordingly, combination of the impedance-matched condition and multiple periodicity quarter-wave stacks allows to design broadband filters which transmit electromagnetic (EM) waves at normal incidence, while reflect all EM waves for larger incidence angles.

The geometry of the proposed solar filter is shown in Figure 1b. It is composed of N Bragg sub-filters of different periodicities ($l_1 \leq l_i \leq l_N$). Each quarter-wave stack consist of M bilayers (unit cells) with defined periodicity according to Bragg's diffraction condition, i.e., the thickness of each layer times its refractive index equals one quarter of the diffracted wavelength. Consequently, the width of the principal stop-band of each stack depends on the ratio of the refractive indices between the two components and is proportional to the diffracted frequency.[15, 16] As an example, the i-th quarter-wave stack is zoomed in Figure 1b. Its thickness is Ml_i, where $l_i = t_1 + t_2$ is the period of the i-th unit cell. The thicknesses of layer 1 (in blue) and layer 2 (in green) are t_1 and t_2, respectively. The thickness of the i-th period is defined by $l_i = l_0 r^{i-1}$, where $l_1 = l_0$ is the starting period of the filter and $r = t_2/t_1$ is ratio between the thicknesses of the two layers forming the unit cell and is constant for all stacks of the filter. It has been shown in literature that increasing the periodicity using a geometrical progression, provides comparable results as choosing each periodicity from a nonlinear optimization algorithm for a given broadband spectrum.[9]

Using the presented concept, we model a filter such that layer 1 is impedance-matched with layer 2 and with the surrounding air ($Z_1 = Z_2 = Z_0$). Accordingly, we set $\epsilon_1 = \mu_1 = 1$ and $\epsilon_2 = \mu_2 = 2$ for layers 1 and 2, respectively. In all cases, the transmittance has been computed using the Transfer-Matrix Method (TMM).[12, 13]

View Article Online
DOI: 10.1039/C9NA00557A 3

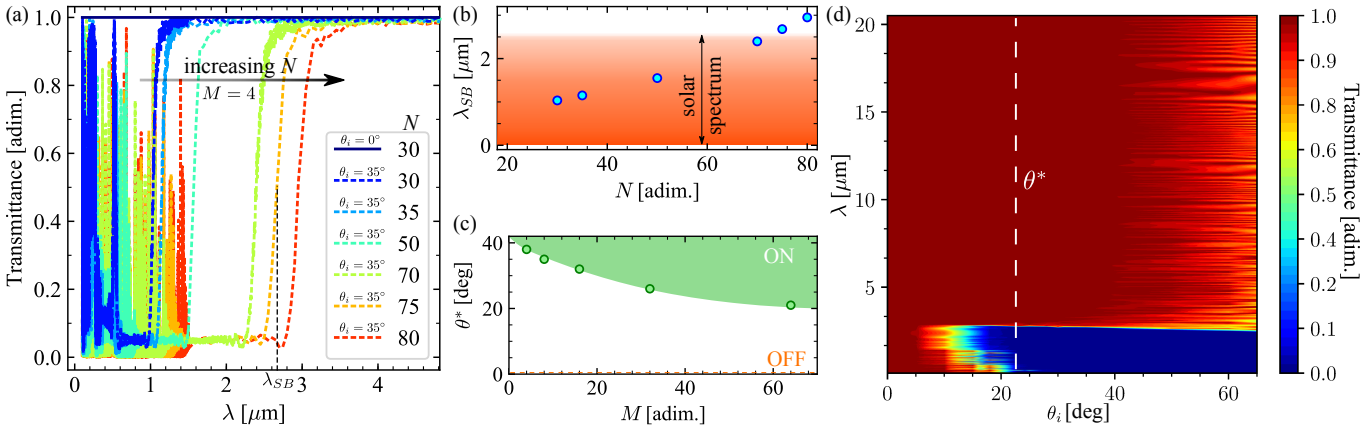

FIG. 2. (a) Exemplary transmittance spectra for different number of quarter-wave stacks at constant number of unit-cells ($M = 4$). (b) Shift of the stop-band wavelength as a function of the number of quarter-wave stacks N. (c) Dependence of the optimum operation angle θ^* of the filter on the number of unit-cells for $N = 75$. (d) Chart of the transmittance spectra for an angle selective solar filter with $N = 75$ and $M = 64$. The dashed vertical line indicates the operation angle of this filter. Note that transmittance is zero in the whole solar spectrum and sharply increases to its maximum value for $\lambda > 2.6$ μm.

Tailoring the solar spectrum

Figure 2a shows the effect of increasing the total number of stacks N in the filter. The larger the number of stacks, the longer the stop-band wavelength λ_{SB} of the filter. We have defined λ_{SB} as the wavelength at which the transmittance of the filter equals 0.5 when the filter is active. The filter is said to be active or ON when it does not transmit any light up to its stop-band wavelength, but transmits all light above this wavelength. In contrast, the filter is OFF when it transmits all light at any wavelength, as shown in Figure 2a by the dark blue spectrum ($\theta_i = 0\,^\circ$). Due to the fact that λ_{SB} is almost independent of the incidence angle when the filter is ON (as confirmed in Figure 2d), any particular selection of θ_i, which makes the filter ON, is valid to explore the effect of increasing the number of quarter-wave stacks (N) for shifting λ_{SB} to longer wavelengths.

Accordingly, in Figure 2a, we have fixed the incidence angle to 35 °, to explore the shift of the stop-band wavelength for $30 \leq N \leq 80$. Even though, this is not the optimum angle for operation of these filters, is a good choice to guaranty that the filters are active, as shown by their corresponding spectra. The stop-band wavelength as a function of the total number of stacks for $M = 4$ unit-cells in each stack, $r = 1.02$ and $l_0 = 200$ nm, is shown in Figure 2b. It shows a nonlinear dependency on N, because the stop-band frequency of each stack is proportional to its mid-gap frequency. This changes according to the previously defined geometrical progression ($l_i = l_0 r^{i-1}$).[11, 15] To cover the entire solar spectrum, we have chosen $N = 75$ stacks for the filter, as indicated in Figure 2b.

Tailoring the angle-selectivity

How many unit-cells should be included in each of the N Bragg-stacks? For this, we explore the effect of the number of unit-cells M in the transmittance spectrum of a filter with $N = 75$, $r = 1.02$ and $l_0 = 200$ nm, which has been optimized for the solar spectrum. We define the optimum operation angle θ^*, as the minimum incidence angle for which transmittance is zero in the solar spectrum, but all radiation is transmitted for wavelengths larger than $\lambda_{SB} = 2.6$ μm. Figure 2c shows that increasing the number of unit-cells M in each stack, reduces θ^*. This is in agreement with the fact that the reflectivity of a 1D photonic crystal reaches the ideal value of 1 when increasing the number of unit-cells or when increasing the incidence angle.[10, 17] Naturally, in this case, increasing the number of unit-cells, means that the maximum reflectivity (zero transmittance) can be achieved at smaller incidence angles. Accordingly, an optimum incidence angle $\theta^* = 23\,^\circ$ was obtained for $M = 64$. This is indicated in Figure 2d with a vertical dashed line.

Figure 2d shows that for normal incidence ($\theta_i = 0\,^\circ$) all radiation is transmitted in the spectrum $0.1 \leq \lambda \leq 20.5$ μm and the filter is OFF. The OFF state is indicated by the dashed line in Figure 2c. For incidence angles $0 < \theta_i < \theta^*$, the filter is ON, but only larger wavelengths within the solar spectrum are reflected, while all other radiation is transmitted. This is because the edges of the band gaps for 1D photonic crystals shift to higher frequencies (short wavelengths) when increasing the incidence angle.[11, 18] On the other hand, for incidence angles $\theta_i > \theta^*$, the filter is ON and the the entire spectrum of solar radiation is reflected. In this case, all radiation with wavelength larger than $\lambda_{SB} = 2.6$ μm is transmitted. Nevertheless, for $\theta_i \gtrsim 40\,^\circ$, the presence of interference reduces the total transmitted radiation.

View Article Online
DOI: 10.1039/C9NA00557A 4

For this reason, the optimum performance of the filter is obtained for incidence angles $\theta^* \leq \theta_i \lesssim 40\,^\circ$. In this range of incidence angles, the whole solar radiation is fully reflected and all radiation within the sky-window ($7.5 \leq \lambda \leq 14$ μm) is completely transmitted. It's worth to point out that θ^* does not mark a critical angle, but instead a threshold angle for the optimum operation of the filter. More details about the designed filter are provided in the supplementary information.[19]

Such a filter is challenging to construct in the laboratory. On the one hand, layer 1 needs a refractive index close to air ($n_1 = 1$) over the whole wavelength range. Recently, nano and microstructured photonic materials have shown to be appropriate to meet the optical properties required for impedance-matching to air in a broadband spectrum. In particular, 3D thin-shell nanolattices made out of Al_2O_3 or ZnO have shown refractive indices around 1.025 in a broadband spectrum.[20] Additionally, arrays of SiO_2 nanorods have shown low refractive indices down to 1.08. Similarly, phase separation of nanoporous thin polymer films (PMMA-PS) has also shown low refractive indices down to 1.05.[21, 22] On the other hand, layer 2 requires a refractive index $n_2 = 2$ over the same wavelength range. This could be realized by nanocomposites comprising high refractive index polymers, such as recently discovered sulfur-based polymers,[23] and high refractive index inorganic nanoparticles such as boron nitride or titania. A further difficulty represents the necessity to fabricate such promising refractive index optimized structures into thin films of high quality.

ENERGY BALANCE OF A FILTER-RADIATIVE COOLER SYSTEM

We now investigate the integration of such an angle-selective filter into passive daytime cooling device. We propose an angle-selective solar filter on top of a nocturnal radiative cooler (radiator), as shown in Figure 3a. The radiator consists of a photonic solar absorber covered by a transparent thermal blackbody and its spectral emissivity is plotted in the supplementary information.[19] The air gap between the nocturnal radiator and the filter is larger than the wavelengths of the incident radiation, i.e., much larger than 20 μm. The operation principle of this device is controlled by the filter: when the filter is OFF (normal incidence), radiative cooling is overwhelmed by solar radiation heating. Therefore, the radiator will be heated up, since its emissivity (absorbance) is non zero in the solar spectrum. On the other hand, when the filter is at its optimum operation angle ($\theta_i = \theta^*$), maximum cooling is obtained from this device. The power balance between the filter-radiator system can be expressed as a pair of coupled integro-differential equations:[19, 24]

$$P_{total,rad} = P_{sun} + P_{atm}(T_{amb}) + P_{conv}(T, T_{fil}) + P_{exc}(T, T_{fil}) - P_{dev}(T), \quad (1)$$

$$P_{total,fil} = P_{sun,fil} + P_{atm,fil}(T_{amb}) + P_{conv,fil}(T, T_{fil}, T_{amb}) - P_{exc}(T, T_{fil}) - P_{dev}(T) - P_{fil}(T_{fil}), \quad (2)$$

where the total cooling power per unit area of the radiator is given by $P_{total,rad} = \rho_{rad} c_{rad} / A_{rad}\,(\mathrm{d}T/\mathrm{d}t)$ and the total cooling power per unit area of the filter is $P_{total,fil} = \rho_{fil} c_{fil} / A_{fil}\,(\mathrm{d}T_{fil}/\mathrm{d}t)$. The density and specific heat capacity of each component are represented by ρ_x and c_x, respectively. Similarly, A_x stands for the surface area of each component under normal incidence of solar radiation. The sub-index $x = \{rad, fil\}$ labels each component. T_{amb} is the ambient temperature of the surroundings.

A radiative cooling system as the one in Figure 3a, can only supply sensible cooling if $P_{dev}(T = T_{amb})$ exceeds all incoming heating at the initial T_{amb} (see Equation 1). In this case, as time passes, the radiator temperature drops below the ambient temperature, down to a steady state temperature T.[1, 6] When the steady state is reached, the filter-radiator system is in thermal equilibrium with the surroundings. Therefore, the total energy of both the radiator and the filter must remain constant. This implies that the total cooling power (derivative of the energy with respect to time) of the radiator and the filter goes to zero, i.e., $P_{total,rad} = P_{total,fil} = 0$. Consequently, the system of Equations (1) and (2) simplifies into a pair of simultaneous homogeneous equations.[25] This system can be solved numerically to obtain the temperature of the radiator (T) and the temperature of the filter (T_{fil}).

The total cooling power of the radiator presented in Equation (1) is equal to the absorbed power from the solar radiation P_{sun}, the radiatively absorbed power from the surrounding atmosphere $P_{atm}(T_{amb})$, the convective power between the air gap and the (upper) surface of the radiator $P_{conv}(T, T_{fil})$, the radiative power exchanged from the bottom surface of the filter to the surface of the radiator $P_{exc}(T, T_{fil})$ and the negative of the power emitted by the device $P_{dev}(T)$. This is the power emitted by the combined radiator-filter system to the outer space through the atmospheric windows, when the radiator surface is at temperature T. Accordingly, $P_{dev}(T)$ is the actual cooling power of the radiator surface in presence of the filter. These radiative powers have been computed taking into account the presence of the filter on top of the radiator.

Similarly, the total cooling power of the filter given in Equation (2) is equal to the absorbed power from the solar radiation $P_{sun,fil}$, the radiatively absorbed power from the surrounding atmosphere $P_{atm,fil}(T_{amb})$, the convective power from the surrounding air to the upper surface of the filter and between the air gap and the bottom surface of the filter $P_{conv,fil}(T, T_{fil}, T_{amb})$, the

View Article Online
DOI: 10.1039/C9NA00557A 5

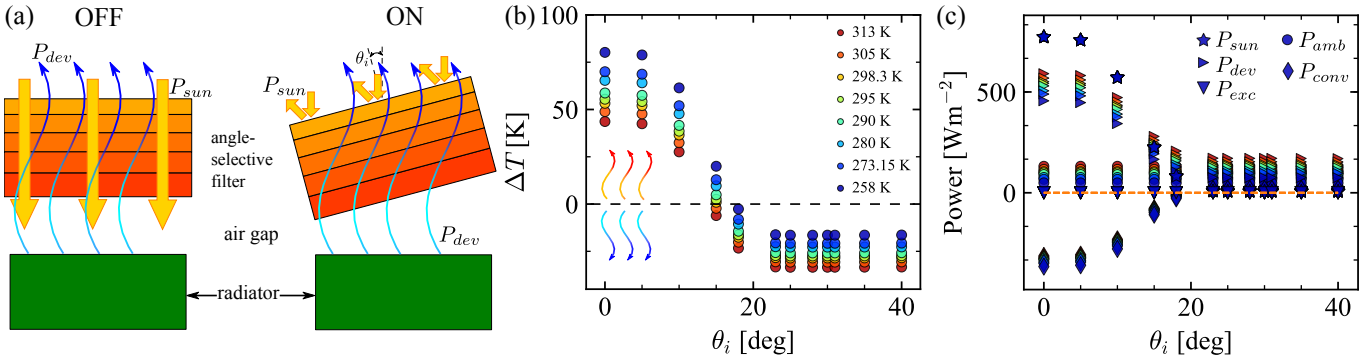

FIG. 3. (a) Diagram of the proposed radiator-filter device. Under normal incidence the solar filter is OFF, but it is turned ON by tilting it. The radiator is able to cool itself when the filter reflects all the solar radiation. (b) Temperature difference ($\Delta T = T - T_{amb}$) between the radiator surface and the ambient as a function of the incidence angle. Positive values mean that the radiator is being heated, while negative values refer to the cooling of the radiator surface. (c) Computed power contributions per unit area for the radiator, see Equation (1), as a function of the incidence angle. The maximum net cooling is obtained for $\theta_i \geq 23\,^\circ$ and is around 140 Wm^{-2}. All calculations are performed assuming steady-state conditions.

negative of the radiative power exchanged from the bottom surface of the filter to the surface of the radiator $P_{exc}(T, T_{fil})$, the negative of the intrinsic power emitted by the device $P_{dev}(T)$ and the negative of the power emitted by the upper surface of the filter $P_{fil}(T_{fil})$.

From Equation (1), P_{sun} is the input power per unit area from the sun to the radiator screened by the filter. This means that the emissivity of the combined filter-radiator is used: $\epsilon_{dev}(\lambda) = t_{fil}(\lambda)\frac{1-r_{rad}(\lambda)}{1-r_{fil}(\lambda)r_{rad}(\lambda)}$, being $r_{rad}(\lambda) = 1 - \epsilon_{rad}(\lambda)$. Accordingly: $P_{sun} = \int_0^\infty I_{AM1.5}(\lambda)\epsilon_{dev}(\lambda)\mathrm{d}\lambda$, where $I_{AM1.5}(\lambda)$ is the spectral irradiance of the sun.[26] $\epsilon_{rad}(\lambda)$ stands for the angle averaged emissivity of the radiator. This assumption is valid, since it is well-known that the angle dependency of the emissivity of a nocturnal radiator surface slightly decreases for large incidence angles ($\theta_i > 70\,^\circ$).[2, 7] On the other hand, the emissivity of the device depends on the incidence angle, because the transmittance of the filter is a function of the incidence angle θ_i. Consequently, P_{sun} is also a function of the incidence angle.

The input power from the atmosphere to the radiator in presence of the filter is $P_{atm}(T_{amb}) = \pi \int_0^\infty \int_0^{\pi/2} I_{BB}(T_{amb}, \lambda)\epsilon_{dev}(\lambda)\epsilon_{atm}(\lambda, \theta) \sin 2\theta \mathrm{d}\theta\mathrm{d}\lambda$, where the emissivity of the atmosphere is computed as $\epsilon_{atm}(\lambda, \theta) = 1 - [1 - t_{atm}(\lambda, 0\,^\circ)]^{1/\cos\theta}$ and $t_{atm}(\lambda, 0\,^\circ)$ is the transmittance spectrum of the atmosphere at zenit.[27] $I_{BB}(T, \lambda)$ represents the blackbody spectral irradiance at the specified temperature, according to Planck's law.

The convective loss in the upper radiator surface due to the air gap between the radiator and the filter is $P_{conv}(T, T_{fil}) = h_{conv}\,[(T + T_{fil})/2 - T]$, where h_{conv} is the heat transfer coefficient due to convection to the surrounding air. The air gap temperature is considered as the mean value between the temperature of the radiator T and the temperature of the filter T_{fil}. A typical value of the heat transfer coefficient due to natural convection ($h_{conv} = 8$ Wm^{-2}K^{-1}) has been used for all calculations.[1]

Heat conduction to the surrounding air can be neglected in the limit of low humidity in the atmosphere. However, for situations in which this approximation is not fulfilled (high humidity), Equations (1) and (2) turns into a pair of coupled conductive-convective-radiative integro-differential equations.[28]

The exchanged power by radiation between the radiator surface and the bottom surface of the filter is $P_{exc}(T, T_{fil}) = \pi \int_0^\infty \frac{[I_{BB}(T_{fil},\lambda) - I_{BB}(T,\lambda)]\epsilon_{fil}(\lambda)\epsilon_{rad}(\lambda)}{\epsilon_{fil}(\lambda)+\epsilon_{rad}(\lambda)-\epsilon_{fil}(\lambda)\epsilon_{rad}(\lambda)}\mathrm{d}\lambda$, where $\epsilon_{rad}(\lambda)$ and $\epsilon_{fil}(\lambda)$ are the spectral emissivities of the radiator and the filter, respectively.

The cooling power of the device, i.e., the radiator in presence of the filter, is given by: $P_{dev}(T) = \pi \int_0^\infty I_{BB}(T, \lambda)\epsilon_{dev}(\lambda)\mathrm{d}\lambda$. The corresponding power expressions for the filter are provided in the supplementary information.[19]

TUNABLE DAYTIME PASSIVE RADIATIVE COOLING

The filter shown in Figure 3a is an angle-selective solar filter with $N = 75$ and $M = 64$, which was studied above. The radiator is a solar absorber covered by a visibly transparent thermal blackbody, based on a silica photonic crystal.[2] We have chosen such a radiator to prove that is possible to achieve tunable daytime passive radiative cooling with the proposed filter-radiator device. Another radiator configurations with distinct spectral properties are given in the supporting information (Figure S4).[19] The operation principle of the radiator-filter device is that heating or cooling can be tuned by simply tilting the angle-selective solar filter. Nevertheless, the angular location of the sun must be considered when selecting the appropriate tilting angle of the filter. This is because, the incidence angle (θ_i) is the relative

View Article Online
DOI: 10.1039/C9NA00557A 6

angle between the solar radiation and the normal to the surface of the filter.

Figure 3b shows the temperature difference between the radiator surface and the ambient ($\Delta T = T - T_{amb}$) as a function of the incidence angle θ_i. Eight different values of ambient temperature (color coded) have been studied to cover a wide range of typical situations. All calculations assume steady-state conditions.

The temperature difference ΔT is positive at incidence angles lower than 15 °. This means that the radiator is being heated because all (normal incidence) or part of the solar radiation reaches the radiator surface. In this case, the cooling power emitted through the sky-window is not enough to overcome the heating induced by the incident solar radiation. On the other hand, for larger incidence angles ($\theta_i > 15\,°$), ΔT is zero or negative, which indicates that the radiator can cool itself, by emitting radiation through the sky-window, down to temperatures equal or lower than the ambient temperature. Due to the fact that the filter can only reflect the entire spectrum of solar radiation for incidence angles $\theta_i \leq \theta^*$, the lowest temperature this radiator can reach is obtained for incidence angles larger or equals to 23 °. The lowest radiator temperature reached with this device is around 270 K and the maximum temperature is 351.6 K. Accordingly, we have shown that it is possible to tune between heating and cooling (or vice versa) of the radiator in a wide range of temperatures by changing the incidence angle between the sun radiation and the filter.

Figure 3c shows the power contributions per unit area for the nocturnal radiator as a function of the incidence angle. Each contribution appearing in Equation (1) is represented. Results for the eight different ambient temperatures studied in Figure 3b are displayed (same color code). The cooling power of the radiator (right triangles) obtained for $\theta_i \geq 23\,°$ is around 140 Wm^{-2}.[1, 29] This gives the lowest temperature of the radiator.

The incident radiation from the sun to the radiator (star markers) is reduced from 772.6 Wm^{-2} down to around 7 Wm^{-2} by changing the incidence angle from normal incidence to $\theta_i \geq 23\,°$, respectively. This reduction is independent of the ambient temperature, as expected. The incident power from the atmosphere to the radiator (dot markers) is almost independent of the incidence angle and only changes slightly with the ambient temperature. This is because the emissivity of the atmosphere only show significant changes for incidence angles larger than 60 °. The radiative exchange power between the filter and radiator surfaces (downwards triangles) is zero for all incidence angles, which agrees with the steady-state condition. The convective power (diamond markers) between the air gap and radiator changes from a cooling mechanism ($T > T_{amb}$) to a heating source ($T < T_{amb}$) for the radiator surface. The sum of terms on the right hand side of Equation (1) is represented by the dashed line. $P_{total,rad} = 0$ for any incidence angle, as expected in the steady-state regime. More details are given in the supplementary information.[19]

CONCLUSION

In this work we have shown that tunable daytime passive radiative cooling is possible by using an angle-selective solar filter on top of a nocturnal radiative cooler surface. We have provided guidelines for the design of such an angle-selective solar filter, based on a one-dimensional photonic crystal composed of multiple Bragg-stacks with different periodicities designed to cover the entire solar spectrum. We have shown that the proposed device operates at its maximum performance for incidence angles equal to or larger than 23 °. The surface temperature of the radiator can be controlled from 270 K to 352 K in an atmosphere of 298.3 K, with a maximum net cooling power ~ 140 Wm^{-2}. This is comparable to the optimum performance of static devices. Our findings show that the proposed filter-radiator concept is promising for active control of daytime passive radiative cooling.

CONFLICTS OF INTEREST

There are no conflicts to declare.

ACKNOWLEDGMENT

Support by the Bavarian Polymer Institute and the SFB840 is acknowledged.

Funding Sources

This project has received funding from the European Research Council (ERC) under the European Unions Horizon 2020 research and innovation program (grant agreement No 714968).

* nelson.pech@uni-bayreuth.de
† markus.retsch@uni-bayreuth.de

[1] M. M. Hossain and M. Gu, Adv. Sci. **3**, 1500360 (2016).
[2] L. Zhu, A. P. Raman, and S. Fan, Proc. Natl. Acad. Sci. U. S. A. **112**, 12282 (2015).
[3] J. Mandal, Y. Fu, A. C. Overvig, M. Jia, K. Sun, N. N. Shi, H. Zhou, X. Xiao, N. Yu, and Y. Yang, Science **362**, 315 (2018).
[4] E. Rephaeli, A. Raman, and S. Fan, Nano Lett **13**, 1457 (2013).
[5] Y. Zhai, Y. Ma, S. N. David, D. Zhao, R. Lou, G. Tan, R. Yang, and X. Yin, Science **355**, 1062 (2017).
[6] S. Catalanotti, V. Cuomo, G. Piro, D. Ruggi, V. Silvestrini, and G. Troise, Solar Energy **17**, 83 (1975).

View Article Online
DOI: 10.1039/C9NA00557A 7

[7] C. G. Granqvist and A. Hjortsberg, J. Appl. Phys. **52**, 4205 (1981).
[8] T. Li, Y. Zhai, S. He, W. Gan, Z. Wei, M. Heidarinejad, D. Dalgo, R. Mi, X. Zhao, J. Song, J. Dai, C. Chen, A. Aili, A. Vellore, A. Martini, R. Yang, J. Srebric, X. Yin, and L. Hu, Science **364**, 760 (2019).
[9] Y. Shen, D. Ye, I. Celanovic, S. G. Johnson, J. D. Joannopoulos, and M. Soljacic, Science **343**, 1499 (2014).
[10] J. N. Winn, Y. Fink, S. Fan, and J. D. Joannopoulos, Opt. Lett. **23** (1998).
[11] X. Wang, X. H. Hu, Y. Z. Li, W. L. Jia, C. Xu, X. H. Liu, and J. Zi, Appl. Phys. Lett. **80**, 4291 (2002).
[12] M. Born and E. Wolf, *Principles of Optics: Electromagnetic Theory of Propagation, Interference and Diffraction of Light*, 6th ed. (Elsevier Science Limited, 1980).
[13] R. C. Rumpf, Prog. Electromagn. Res. B **35**, 241 (2011).
[14] J. D. Jackson, *Classical electrodynamics*, 3rd ed. (Wiley, New York, NY, 1999).
[15] J. Lekner, J. Opt. A: Pure Appl. Opt. **2**, 349 (2000).
[16] J. Joannopoulos, S. Johnson, J. Winn, and R. Meade, *Photonic Crystals: Molding the Flow of Light - Second Edition* (Princeton University Press, 2011).
[17] P. Yeh, A. Yariv, and C.-S. Hong, J. Opt. Soc. Am. **67** (1977).
[18] W. H. Southwell, Appl. Opt. **38** (1999).
[19] See supplementary information at (link) for details on the filter geometrical parameters, exemplary transmission spectra of the filter, diagram of energy balance for the radiator and filter, power expressions for the filter, spectral properties of the radiator, solar spectral irradiance, atmospheric transmittance, numerical results of the computed temperatures and powers for two extreme cases of ideal radiators.
[20] X. A. Zhang, A. Bagal, E. C. Dandley, J. Zhao, C. J. Oldham, B.-I. Wu, G. N. Parsons, and C.-H. Chang, Adv. Funct. Mater. **25**, 6644 (2015).
[21] J. Q. Xi, J. K. Kim, E. F. Schubert, D. Ye, T. M. Lu, S.-Y. Lin, and J. S. Juneja, Opt. Let. **31** (2006).
[22] S. Walheim, E. Schffer, J. Mlynek, and U. Steiner, Science **283**, 520 (1999).
[23] T. S. Kleine, N. A. Nguyen, L. E. Anderson, S. Namnabat, E. A. LaVilla, S. A. Showghi, P. T. Dirlam, C. B. Arrington, M. S. Manchester, J. Schwiegerling, R. S. Glass, K. Char, R. A. Norwood, M. E. Mackay, and J. Pyun, ACS Macro Lett. **5**, 1152 (2016).
[24] D. Winter, Int. J. Heat Mass Tran. **9**, 527 (1966).
[25] S. A. Dyakov, J. Dai, M. Yan, and M. Qiu, Phys. Rev. B **90**, 045414 (2014).
[26] ASTM G173-03, *Standard Tables for Reference Solar Spectral Irradiances: Direct Normal and Hemispherical on 37° Tilted Surface*, Standard (ASTM International, West Conshohocken, PA, 2012).
[27] A. Berk, G. P. Anderson, P. K. Acharya, L. S. Bernstein, L. Muratov, J. Lee, M. Fox, S. M. Adler-Golden, J. H. Chetwynd Jr., M. L. Hoke, R. B. Lockwood, J. A. Gardner, T. W. Cooley, C. C. Borel, P. E. Lewis, and E. P. Shettle, in *Algorithms and Technologies for Multispectral, Hyperspectral, and Ultraspectral Imagery XII*, Vol. 6233, edited by S. S. Shen and P. E. Lewis (SPIE, 2006).
[28] D. Maillet, S. André, J. C. Batsale, A. Degiovanni, and C. Moyne, *Thermal quadrupoles: solving the heat equation through integral transforms*, Loyola Symposium Series (Wiley, 2000).
[29] S. Buddhiraju, P. Santhanam, and S. Fan, Proc. Natl. Acad. Sci. U. S. A. (2018).

TABLE OF CONTENTS

View Article Online
DOI: 10.1039/C9NA00557A

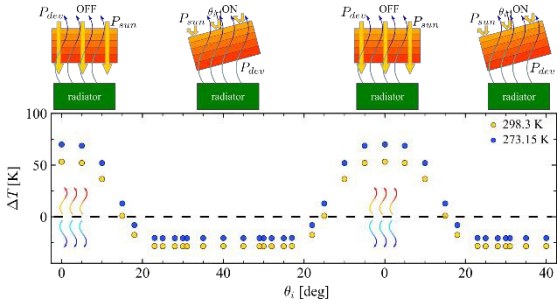

Dynamic control for passive radiative cooling during daytime.